

Giant offshore pumice deposit records a shallow submarine explosive eruption of ancestral Santorini

Supplementary Information

Tim Druitt¹, Steffen Kutterolf², Thomas A. Ronge³, Christian Hübscher⁴, Paraskevi Nomikou⁵, Jonas Preine⁴, Ralf Gertisser⁶, Jens Karstens², Jörg Keller⁷, Olga Koukousioura⁸, Michael Manga⁹, Abigail Metcalfe¹, Molly McCanta¹⁰, Iona McIntosh¹¹, Katharina Pank², Adam Woodhouse¹², Sarah Beethe¹³, Carole Berthod¹⁴, Shun Chiyonobu¹⁵, Hehe Chen¹⁶, Acacia Clark¹⁷, Susan DeBari¹⁸, Raymond Johnston¹⁹, Ally Peccia²⁰, Yuzuru Yamamoto²¹, Alexis Bernard²², Tatiana Fernandez Perez²³, Christopher Jones²⁴, Kumar Batuk Joshi²⁵, Günther Kletetschka²⁶, Xiaohui Li²⁷, Antony Morris²⁸, Paraskevi Polymenakou²⁹, Masako Tominaga³⁰, Dimitrios Papanikolaou⁵, Kuo-Lung Wang³¹, Hao-Yang Lee³¹

¹University Clermont-Auvergne, CNRS, IRD, OPGC, Laboratoire Magmas et Volcans, Clermont-Ferrand, France

²GEOMAR Helmholtz Centre for Ocean Research Kiel, Wischhofstrasse 1-3, D-24148 Kiel, Germany

³International Ocean Discovery Program, Texas A&M University, College Station TX 77845, USA

⁴Institute of Geophysics, University of Hamburg, Bundesstrasse 55, D-20146 Hamburg, Germany

⁵Department of Geology and Geoenvironment, National and Kapodistrian University of Athens, 15784 Athens, Greece

⁶School of Geography, Geology and the Environment, Keele University, Keele, Staffordshire ST5 5BG, UK

⁷Institut für Geo- und Umweltwissenschaften, Mineralogie - Petrologie, Albertstraße 23b, 79104 Freiburg, Germany

⁸School of Geology, Aristotle University of Thessaloniki, 54124 Thessaloniki, Greece

⁹Department of Earth and Planetary Science, University of California, Berkeley, CA 94720, USA

¹⁰Department of Earth and Planetary Sciences, University of Tennessee, Knoxville TN 37996-1526, USA

¹¹Japan Agency for Marine-Earth Science and Technology, 2-15 Natsushima-cho, Yokosuka Kanagawa 237-0061, Japan

¹²Institute for Geophysics, University of Texas, J.J. Pickle Research Campus, Bldg. 196, Austin TX 78758, USA

¹³College of Earth, Ocean, and Atmospheric Sciences, Oregon State University, Corvallis OR 97333, USA

¹⁴Institut De Physique Du Globe De Paris, Centre National de la Recherche Scientifique (CNRS), 75005 Paris, France

¹⁵Faculty of International Resource Sciences, Akita University, Akita, Akita Prefecture 0108502, Japan

¹⁶School of Ocean Sciences, China University of Geosciences, 100083 Haidan District, Beijing, China

¹⁷School of Natural Sciences/CODES, University of Tasmania, Hobart 7005, Australia

¹⁸Geology Department, Western Washington University, Bellingham WA 98225, USA

¹⁹School of Geosciences, University of South Florida, Tampa FL 33620, USA

²⁰Lamont-Doherty Earth Observatory, Columbia University, Palisades NY 10964, USA

²¹Graduate School of Science, Kobe University, 1-1 Rokkodai-cho, Nada-ku, Kobe, Hyogo 657-8501, Japan

²²Laboratoire des Fluides Complexes et leurs Réservoirs, Université de Pau et des Pays de l'Adour, F-64000 Pau, France

²³Department of Geology, Kent State University, 221 McGilvrey Hall, 325 S Lincoln Street, Kent OH 44242, USA

²⁴Department of Earth and Planetary Sciences, University of California, Riverside CA 92506, USA

²⁵Solid Earth Research Group, National Centre for Earth Science Studies, Thiruvananthapuram, Kerala 695011, India

²⁶Geophysical Institute, University of Alaska Fairbanks, 2156 Koyukuk Drive, Fairbanks Alaska 99775, USA

²⁷Key Laboratory of Submarine Geoscience and Prospecting Techniques, Ocean University of China, Qingdao, China

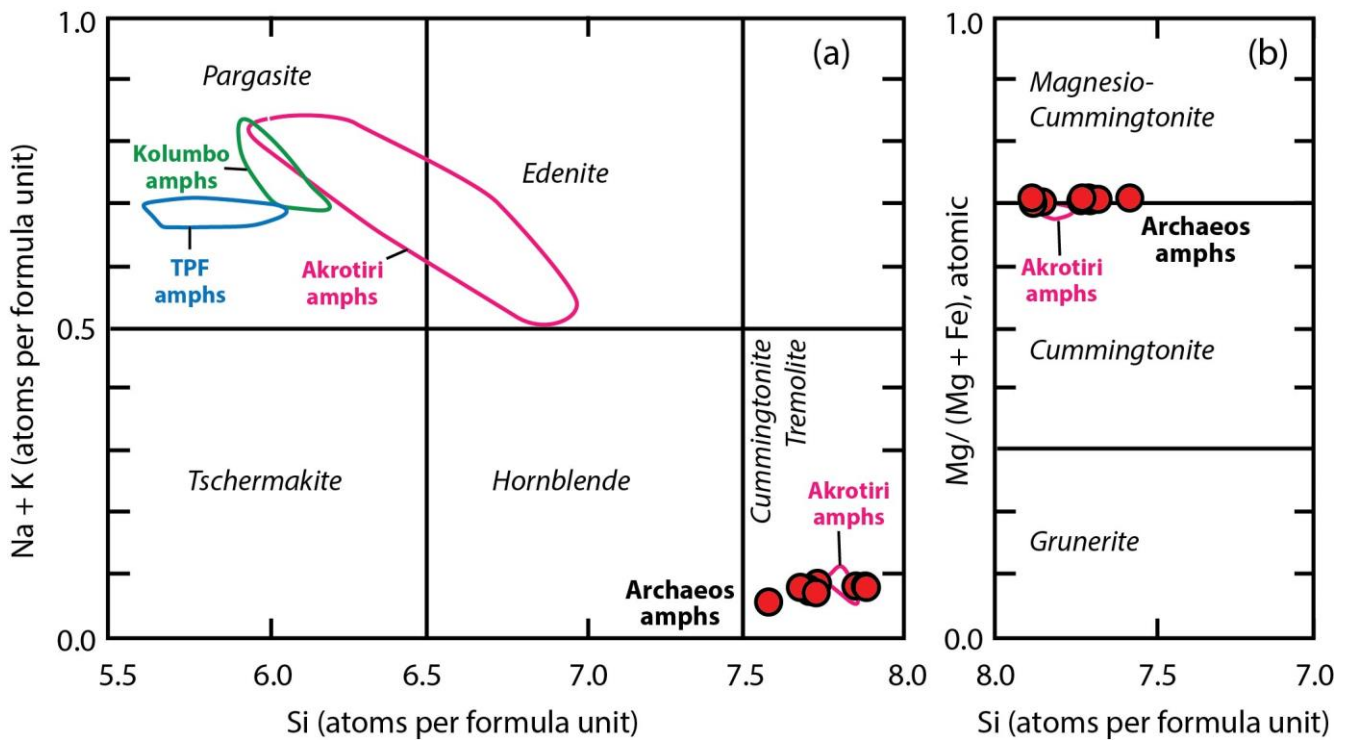
²⁸School of Geography, Earth and Environmental Sciences, Plymouth University, Drake Circus, Plymouth PL4 8AA, UK

²⁹Institute of Marine Biology, Biotechnology and Aquaculture, Hellenic Centre for Marine Research, Heraklion, Greece

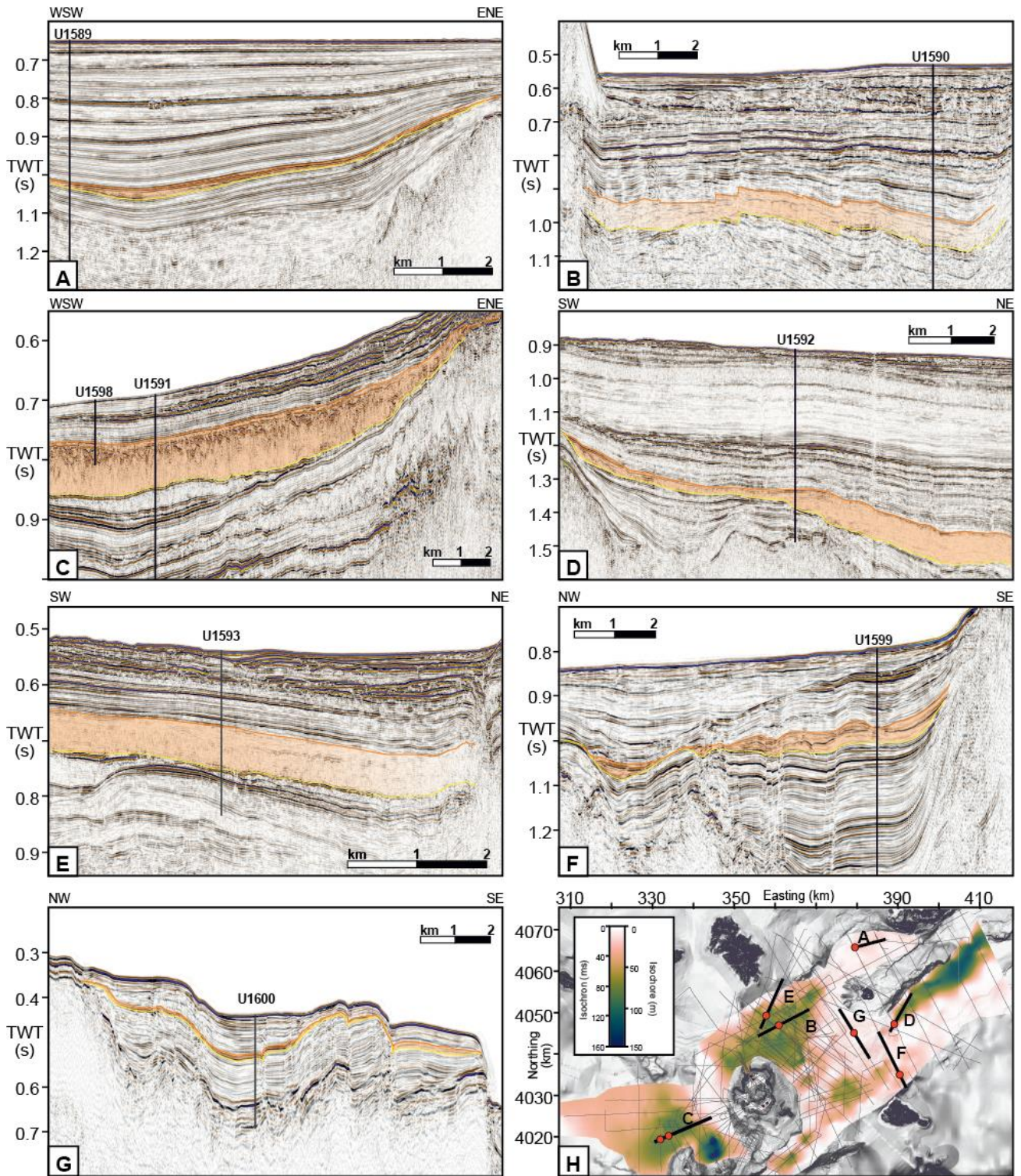
³⁰Department of Geology and Geophysics, Woods Hole Oceanographic Institution, Woods Hole MA 02543, USA

³¹Institute of Earth Sciences, Academia Sinica, Taipei, 11529, Taiwan

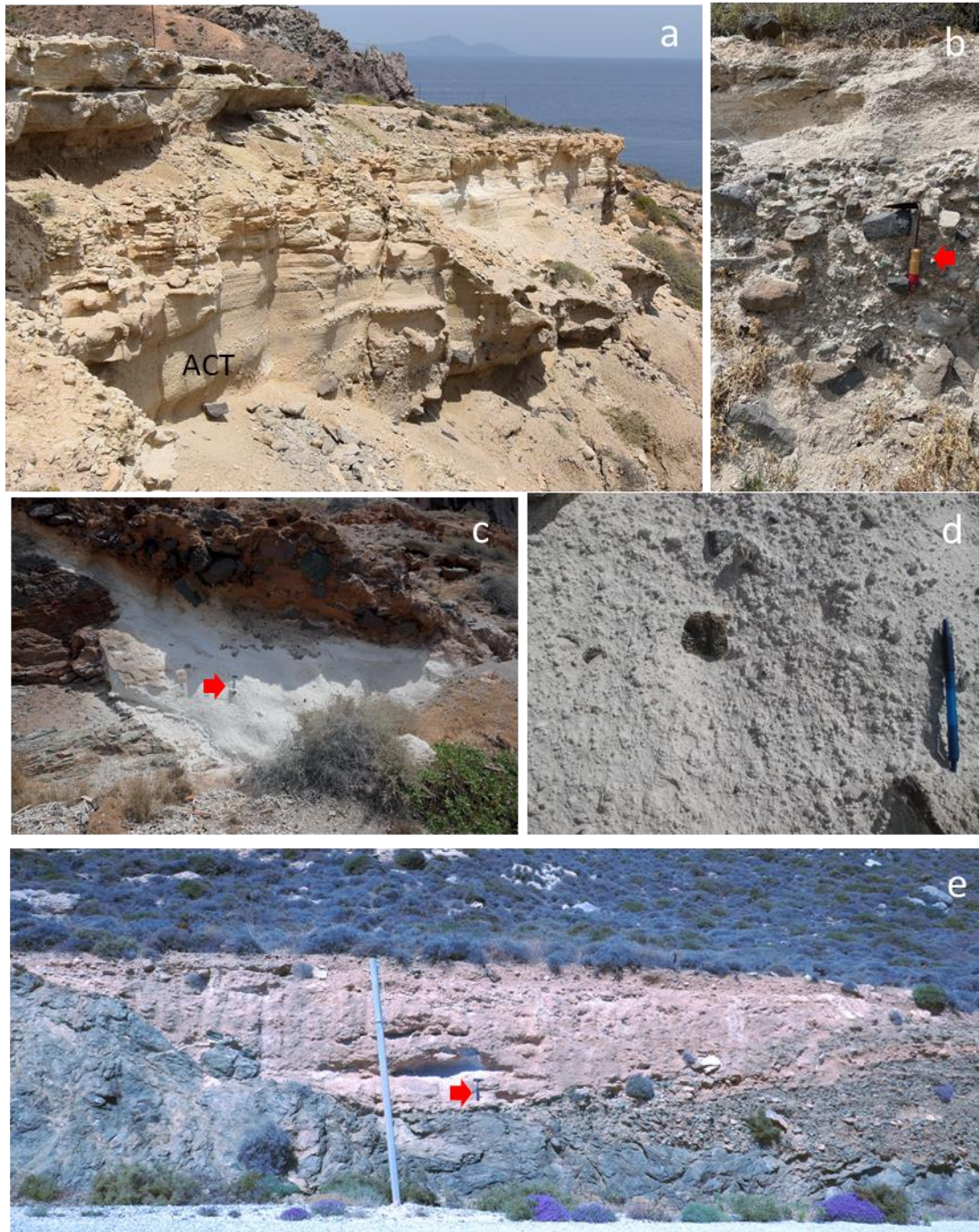
Supplementary figures and tables



Supplementary Figure 1. Amphiboles in the Archaeos Tuff. (a) Compositions of amphiboles (amph) from the Archaeos Tuff, and distinction from those of the Early Centres of Akrotiri^{1,2}, the Thera Pyroclastic Formation (TPF) of Santorini³, and the 1650 CE eruption of Kolumbo⁴. Cummingtonite similar compositionally to that of the Archaeos Tuff occurs in some tuffs of the Akrotiri centres. Note that the Akrotiri tuffs contain coexisting calcic amphiboles and cummingtonite. (b) Classification of the Archaeos amphiboles as cummingtonite to magnesio-cummingtonite, with comparison with those from the Akrotiri centres.



Supplementary Figure 2. Compilation of seismic profiles showing the Archaeos Tuff in orange. Based on published seismic profiles⁵. Note that the unit was not recovered at Site U1590, but its presence is inferred based on the seismic stratigraphy and biostratigraphic age-depth data.



Supplementary Figure 3. Onland outcrops of the Archaeos Tuff. (a) Christiani Island ($36^{\circ}14.74' \text{ N} / 25^{\circ}12.53' \text{ E}$). The Archaeos Tuff (marked ACT) is 4 m thick and is overlain by other minor pumice and ash layers. Santorini lies in the distance. (b) A lithic breccia lens within the Archaeos Tuff on Christiani Island, with scraper for scale (red arrow). (c) The Archaeos Tuff on Santorini. The outcrop occurs near sea level at the base of the caldera wall ($36^{\circ}22.34' \text{ N} / 25^{\circ}25.38' \text{ E}$). The tuff directly overlies basement schists and is in turn overlain by a blocky regolith. The outcrop stratigraphically underlies the entire Thera Pyroclastic Formation of Santorini. Hammer for scale (red arrow). (d) Close-up of the outcrop in Figure c, showing the relatively fine grained and poorly sorted nature of the ignimbrite. (e) Outcrop of the Archaeos Tuff on Anafi Island, where it forms a thin lens directly atop basement schists ($36^{\circ}21.39' \text{ N} / 25^{\circ}48.26' \text{ E}$). Hammer for scale (red arrow). The vertical grey line is a metal pole.

Supplementary Table 1: Description of the submarine facies of the Archaeos Tuff

Thickness	In the cores: thickest (75 m) at Site U1593 and thinnest (6 m) at Site U1600. On seismic images: up to 150 m thick between Santorini and Christiana and in the Anafi Basin.
Grain size	At Sites U1591 and U1598, it is composed of well sorted, clast-supported lapilli tuff poor in fine ash, with pumice lapilli to several cm in diameter. At Site U1589, the deposit is mostly of ash grade.
Texture	Massive to diffusely bedded lapilli-tuff and tuff (terminology of ref 6), with a top that grades up into overlying muds and oozes. Bedding within the deposit reflects variations in grain size and component proportions. Normally graded intervals in some cores may be attributable to sorting within submarine gravity flows, or may be artifacts due to ash liquefaction during drilling and core recovery. Ash liquefaction and other disturbance effects during core recovery (ref 7) overprinted finer-scale sedimentary structures and caused artificial grading within core sections, resulting in loss of sedimentological information.
Consolidation	Totally unconsolidated. The terms lapilli tuff and tuff are used even though the deposit is unconsolidated.
Components	Pumice lapilli, glass shards, lithic fragments and free crystals, with bioclasts picked up from the sea floor
Pumice	The pumice lapilli are highly vesicular and are mostly white, although a subordinate grey variety and white/grey banded varieties are also present. Vesicles in the pumices range from spherical to tubular or fibrous. The pumice lapilli range from angular to rounded.
Lithics	Lithic clasts are systematically smaller than pumice clasts, and occur scattered uniformly throughout the deposit or concentrated in clast-supported lithic-rich layers. Lithic components are mainly lavas, but greenschists, limestone and microgranitoids also occur.

Supplementary Table 2. Grain size analyses of offshore and onshore facies of the Archaeos Tuff

Drill site	Core U1599A	Core U1599A	Core U1599A	Core U1591B	Core U1591B	Core U1599A	Core U1593A	Core U1593A	Core U1598A	Core U1593A	Core U1593B	Core U1593B
Core and section	27F 2	29F 3	29F 2	10F 1	10F 1	28F 3	16H 2	18F 2	09F 2	17F 2	17F 2	27F 2
Depth in section (cm)	46-53	55-63	26-33	89-100	128-138	63-70	95-100	35-40	97-106	30-35	30-35	82-92
64 to 32 mm	-5 phi											
32 to 16 mm	-4 phi											
16 to 8 mm	-3 phi	6.96	6.29	10.34	11.78	7.15	5.38	10.08	2.48	13.12	5.47	0.08
8 to 4 mm	-2 phi	20.45	5.82	21.00	16.54	15.99	6.10	30.59	14.54	28.22	13.12	2.20
4 to 2 mm	-1 phi	27.00	11.68	24.97	18.07	30.24	10.48	29.22	22.21	26.98	21.31	7.98
2 to 1 mm	0 phi	14.56	14.17	17.71	17.47	20.64	13.87	13.46	18.54	14.85	25.41	21.01
1 mm to 500 µm	1 phi	7.57	15.56	14.26	16.30	13.70	15.49	8.09	16.84	9.53	21.84	23.53
500 to 250 µm	2 phi	7.55	17.15	8.37	11.92	7.71	20.27	4.94	13.44	5.69	6.75	24.92
250 to 125 µm	3 phi	7.11	13.82	2.34	5.35	2.50	17.91	2.48	7.31	1.24	3.36	19.54
125 to 63 µm	4 phi	4.47	7.78	0.72	1.37	1.14	6.63	0.74	3.26	0.25	1.36	0.65
<63 µm	>4 phi	4.32	7.72	0.30	1.21	0.94	3.86	0.41	1.38	0.12	1.39	0.08
Inman median (phi units) ⁸	-1.20	0.80	-1.30	-0.80	-1.10	0.90	-1.70	-0.45	-1.70	-0.60	-0.60	0.80
Inman sorting (phi units) ⁸	2.28	2.30	1.70	2.03	1.55	2.08	1.45	1.88	1.50	1.50	1.50	1.44
Wt % < 1 mm	31.03	62.03	25.99	36.14	25.98	64.17	16.66	42.22	16.83	34.69	68.73	68.73
Wt % < 63 µm	4.32	7.72	0.30	1.21	0.94	3.86	0.41	1.38	0.12	1.39	0.08	0.08
Wt % 16-8 mm lithics	0	0	0	19	0	0	0	0	0	0	0	0
Wt % 8-4 mm lithics	0	0	0	15	2	0	0	0	0	0	0	0
Wt % 4-2 mm lithics	0	0	0	0	1	0	0	2	0	8	0	0

Drill site	Core U1593B	Core U1591B	Core U1593A	Core U1600A	Core U1589B	Core U1598B	Core U1593A	Core U1589B	Core U1589B	Onland Santorini	Onland Anafi	
Core and section	10F 2	17F 1	14H 2	06F 1	60F 1	03F 1	20F 2	59F 1	60F 1			
Depth in section (cm)	55-65	90-100	50-55	20-30	15-25	91-101	55-65	70-80	5-10			
64 to 32 mm	-5 phi									2.61	4.24	
32 to 16 mm	-4 phi									9.33	6.50	
16 to 8 mm	-3 phi	9.45	0.12	0.04	0.10	5.84	0.13	0.10	0.02	0.04	13.81	12.71
8 to 4 mm	-2 phi	36.44	20.98	6.54	0.10	19.25	4.50	18.03	7.33	0.04	14.93	14.41
4 to 2 mm	-1 phi	23.62	13.35	6.18	4.33	16.71	15.63	18.95	10.57	2.40	8.17	7.06
2 to 1 mm	0 phi	12.01	12.16	4.49	9.38	9.57	17.62	16.11	6.93	5.61	6.87	7.03
1 mm to 500 µm	1 phi	10.26	7.87	2.87	23.51	8.67	24.24	15.60	4.30	9.02	5.67	7.77
500 to 250 µm	2 phi	5.80	18.00	3.34	23.20	8.08	22.78	15.81	5.34	21.16	5.63	8.99
250 to 125 µm	3 phi	2.43	26.34	17.06	34.43	15.37	13.11	10.23	17.94	27.91	7.21	10.88
125 to 63 µm	4 phi	0.00	1.19	43.00	3.51	11.84	1.85	3.34	27.20	13.70	8.30	2.03
<63 µm	>4 phi	0.00	0.00	16.49	1.44	4.67	0.13	1.82	20.39	20.11	17.47	18.37
Inman median (phi units) ⁸	-1.86	0.48	3.26	1.46	-0.17	0.50	-0.20	2.90	2.30	-0.85	-0.30	
Inman sorting (phi units) ⁸	1.53	2.34	2.15	1.38	2.77	1.60	2.05	2.65	1.85	3.89	4.17	
Wt % < 1 mm	18.49	53.40	82.76	86.08	48.63	62.12	46.81	75.15	91.91	44.28	48.05	
Wt % < 63 µm	0.00	0.00	16.49	1.44	4.67	0.13	1.82	20.39	20.11	17.47	18.37	
Wt % 16-8 mm lithics	0	0	0	0	0	0	0	0	0	0	0	
Wt % 8-4 mm lithics	0	0	0	0	0	0	0	0	0	0	0	
Wt % 4-2 mm lithics	9	0	0	0	0	0	0	0	0	0	0	

Supplementary Table 3. Pumice vesicularities

Sample	% Total	% Connected	% Isolated
398 U1599A 28F 1 W 100/140 a	75.3	65.6	9.7
398 U1599A 28F 1 W 100/140 b	75.3	64.3	11.0
398 U1599A 28F 1 W 100/140 c	67.9	49.5	18.4
398 U1599A 27F CC 10/15 a	80.1	72.0	8.1
398 U1599A 27F CC 10/15 b	80.5	71.1	9.3
398 U1599A 27F CC 10/15 c	83.5	74.9	8.7
398 U1599A 29F 3 W 20/75 a	68.5	55.5	13.0
398 U1599A 29F 3 W 20/75 b	73.2	63.4	9.9
398 U1599A 29F 3 W 20/75 c	77.6	68.4	9.3
398 U1591B 10F 2 W 97/104 a	72.4	57.9	14.5
398 U1591B 10F 2 W 97/104 b	78.7	62.7	16.0
398 U1591B 10F 2 W 97/104 c	75.9	64.7	11.2
398 U1599A 25F CC 14/18 a	73.7	60.4	13.2
398 U1599A 25F CC 14/18 b	77.1	63.1	14.1
398 U1599A 25F CC 14/18 c	78.4	64.5	13.9
398 U1599A 26F 1 W 50/90 a	81.7	75.0	6.7
398 U1599A 26F 1 W 50/90 b	69.8	48.2	21.6
398 U1599A 26F 1 W 50/90 c	75.9	61.0	14.9
Mean	75.9	63.5	12.4
1 Standard deviation	4.4	7.5	3.8

Supplementary Table 4. Representative glass analyses

	Christiani	Santorini	Anafi	U1589	U1591	U1592	U1593	U1598	U1599	U1600
Levels	3	3	1	3	4	2	4	8	15	2
Analyses	21	20	13	43	62	28	54	122	223	23
	Mean	Mean	Mean	Mean	Mean	Mean	Mean	Mean	Mean	Mean
	(±1SD)	(±1SD)	(±1SD)	(±1SD)	(±1SD)	(±1SD)	(±1SD)	(±1SD)	(±1SD)	(±1SD)
Na₂O	4.1 (0.2)*	3.0 (0.3)	4.2 (0.3)	4.1 (0.2)	4.1 (0.2)	4.2 (0.2)	4.1 (0.2)	4.1 (0.2)	4.1 (0.2)	4.1 (0.4)
K₂O	3.4 (0.2)	4.9 (0.2)	3.5 (0.3)	3.5 (0.2)	3.5 (0.2)	3.4 (0.2)	3.3 (0.1)	3.4 (0.2)	3.4 (0.2)	3.6 (0.5)
FeO	0.7 (0.1)	0.7 (0.1)	0.7 (0.1)	0.7 (0.1)	0.7 (0.1)	0.7 (0.1)	0.8 (0.1)	0.7 (0.09)	0.8 (0.1)	0.7 (0.08)
SiO₂	78.3 (0.3)	78.0 (0.2)	77.8 (0.3)	78.1 (0.2)	78.0 (0.3)	78.0 (0.3)	78.1 (0.3)	78.1 (0.2)	77.9 (0.3)	78.0 (0.3)
TiO₂	0.1 (0.02)	0.1 (0.02)	0.1 (0.03)	0.1 (0.03)	0.1 (0.02)	0.1 (0.03)	0.1 (0.03)	0.1 (0.03)	0.1 (0.02)	0.1 (0.02)
MgO	0.1 (0.03)	0.1 (0.03)	0.1 (0.02)	0.1 (0.02)	0.1 (0.03)	0.1 (0.03)	0.1 (0.03)	0.1 (0.03)	0.1 (0.03)	0.1 (0.03)
CaO	0.7 (0.03)	0.7 (0.02)	0.7 (0.07)	0.7 (0.04)	0.7 (0.02)	0.7 (0.06)	0.7 (0.06)	0.7 (0.02)	0.7 (0.07)	0.7 (0.03)
MnO	0.1 (0.03)	0.1 (0.04)	0.1 (0.04)	0.1 (0.04)	0.1 (0.04)	0.1 (0.04)	0.1 (0.04)	0.1 (0.05)	0.1 (0.04)	0.1 (0.04)
Al₂O₃	12.4 (0.2)	12.4 (0.1)	12.8 (0.1)	12.6 (0.1)	12.6 (0.1)	12.6 (0.2)	12.6 (0.1)	12.6 (0.1)	12.7 (0.2)	12.6 (0.1)
P₂O₅	0.04 (0.02)	0.02 (0.03)	0.02 (0.02)	0.02 (0.02)	0.02 (0.02)	0.03 (0.02)	0.02 (0.02)	0.02 (0.02)	0.02 (0.02)	0.02 (0.03)
Analyses	21	20	7	14	20	11	26	43	81	12
Rb	108.2 (11.0)	118.5 (22.8)	92.4 (3.5)	94.7 (6.6)	92.1 (2.0)	94.2 (6.5)	92.4 (5.1)	94.9 (2.6)	92.4 (4.5)	98.5 (5.1)
Sr	40.7 (3.3)	38.4 (3.5)	38.3 (0.9)	40.3 (2.7)	37.8 (1.0)	43.1 (5.2)	38.1 (1.8)	39.4 (1.4)	41.4 (3.9)	40.7 (2.9)
Y	17.7 (1.3)	16.4 (0.9)	16.5 (0.5)	16.7 (1.2)	16.5 (0.4)	17.0 (0.7)	16.3 (1.0)	16.8 (0.6)	16.6 (0.8)	17.5 (0.9)
Zr	65.0 (5.2)	61.2 (3.7)	60.9 (1.7)	62.2 (4.1)	60.5 (1.5)	64.7 (4.4)	59.9 (3.5)	62.1 (2.2)	62.7 (3.8)	64.5 (3.1)
Nb	9.8 (0.7)	9.8 (0.8)	8.7 (0.2)	8.9 (0.6)	8.8 (0.2)	9.0 (0.5)	8.7 (0.5)	9.0 (0.3)	8.8 (0.4)	9.4 (0.4)
Cs	1.4 (0.1)	1.4 (0.1)	1.2 (0.03)	1.2 (0.09)	1.2 (0.03)	1.3 (0.07)	1.2 (0.07)	1.2 (0.04)	1.2 (0.08)	1.3 (0.06)
Ba	809.1 (67.1)	732.6 (47.0)	743.5 (33.3)	767.7 (54.6)	746.1 (19.1)	775.9 (36.5)	744.2 (44.4)	765.9 (25.5)	754.8 (37.8)	799.7 (36.6)
La	24.1 (2.3)	20.5 (1.2)	22.1 (0.8)	22.6 (1.6)	22.0 (0.6)	23.7 (1.5)	21.9 (1.3)	22.5 (0.8)	22.7 (1.4)	23.5 (1.1)
Ce	43.3 (3.4)	39.0 (2.5)	38.9 (1.6)	40.8 (3.0)	39.2 (1.1)	41.7 (2.5)	39.0 (2.5)	40.4 (1.4)	40.3 (2.3)	41.8 (1.9)
Pr	4.1 (0.5)	3.6 (0.2)	3.8 (0.1)	3.9 (0.3)	3.8 (0.1)	4.0 (0.2)	3.7 (0.2)	3.9 (0.1)	3.9 (0.2)	4.0 (0.2)
Nd	13.0 (1.2)	12.0 (0.6)	12.3 (0.6)	13.0 (1.0)	12.5 (0.3)	13.1 (0.7)	12.4 (0.7)	12.8 (0.5)	12.7 (0.8)	13.5 (0.7)
Sm	2.4 (0.3)	2.2 (0.2)	2.3 (0.1)	2.4 (0.2)	2.3 (0.07)	2.4 (0.2)	2.3 (0.2)	2.3 (0.09)	2.3 (0.1)	2.4 (0.1)
Eu	0.4 (0.1)	0.4 (0.06)	0.4 (0.01)	0.4 (0.04)	0.4 (0.02)	0.4 (0.04)	0.4 (0.03)	0.4 (0.03)	0.4 (0.03)	0.4 (0.02)
Gd	2.2 (0.3)	2.1 (0.3)	2.1 (0.1)	2.1 (0.2)	2.1 (0.1)	2.2 (0.1)	2.0 (0.1)	2.1 (0.1)	2.1 (0.1)	2.2 (0.1)
Tb	0.4 (0.06)	0.3 (0.04)	0.4 (0.02)	0.4 (0.03)	0.3 (0.02)	0.4 (0.03)	0.3 (0.02)	0.4 (0.02)	0.4 (0.02)	0.4 (0.02)
Dy	2.6 (0.3)	2.3 (0.3)	2.5 (0.2)	2.5 (0.2)	2.5 (0.09)	2.5 (0.1)	2.4 (0.2)	2.5 (0.1)	2.4 (0.1)	2.6 (0.2)
Ho	0.6 (0.07)	0.5 (0.05)	0.6 (0.02)	0.6 (0.05)	0.5 (0.02)	0.6 (0.03)	0.5 (0.04)	0.6 (0.02)	0.5 (0.04)	0.6 (0.03)
Er	1.9 (0.2)	1.6 (0.1)	1.7 (0.1)	1.8 (0.1)	1.7 (0.06)	1.8 (0.1)	1.7 (0.1)	1.8 (0.07)	1.8 (0.09)	1.9 (0.07)
Tm	0.3 (0.05)	0.3 (0.03)	0.3 (0.02)	0.3 (0.02)	0.3 (0.01)	0.3 (0.02)	0.3 (0.03)	0.3 (0.02)	0.3 (0.02)	0.3 (0.02)
Yb	2.4 (0.3)	2.1 (0.2)	2.3 (0.2)	2.3 (0.2)	2.2 (0.09)	2.3 (0.1)	2.2 (0.2)	2.3 (0.1)	2.2 (0.2)	2.4 (0.1)
Lu	0.4 (0.04)	0.3 (0.03)	0.3 (0.03)	0.4 (0.04)	0.4 (0.02)	0.4 (0.02)	0.4 (0.03)	0.4 (0.02)	0.4 (0.02)	0.4 (0.02)
Hf	2.4 (0.3)	2.1 (0.2)	2.2 (0.1)	2.2 (0.2)	2.1 (0.09)	2.2 (0.1)	2.1 (0.1)	2.2 (0.08)	2.2 (0.1)	2.3 (0.2)
Ta	1.0 (0.2)	0.9 (0.1)	0.8 (0.03)	0.9 (0.07)	0.9 (0.03)	0.9 (0.06)	0.9 (0.06)	0.9 (0.03)	0.8 (0.05)	0.9 (0.05)
Pb	10.0 (1.5)	9.6 (1.6)	9.4 (3.4)	8.3 (0.7)	8.2 (0.2)	8.8 (0.5)	8.2 (0.5)	8.4 (0.4)	8.4 (0.5)	8.6 (0.3)
Th	17.9 (1.5)	16.7 (0.9)	16.6 (0.8)	17.0 (1.4)	16.6 (0.5)	17.1 (0.9)	16.5 (1.0)	16.8 (0.6)	16.6 (0.9)	17.7 (0.9)
U	6.3 (0.6)	6.4 (0.5)	5.5 (0.3)	5.9 (0.5)	5.7 (0.2)	5.8 (0.4)	5.7 (0.4)	5.8 (0.3)	5.7 (0.4)	6.1 (0.3)
Zr/Nb	6.6	6.3	7.0	7.0	6.9	7.2	6.9	6.9	7.2	6.9
Th/Yb	7.5	8.1	7.2	7.4	7.5	7.5	7.4	7.4	7.4	7.5
Ba/Ce	18.7	18.8	19.1	18.8	19.0	18.7	19.1	18.9	18.8	19.1
Zr/Rb	0.6	0.5	0.7	0.7	0.7	0.7	0.6	0.7	0.7	0.7
Ba/Y	45.7	44.5	45.0	45.9	45.2	45.6	45.7	45.5	45.5	45.7
Ba/Rb	7.5	6.4	8.0	8.1	8.1	8.3	8.1	8.1	8.2	8.1
Ce/Gd	20.3	18.7	18.5	20.0	19.0	19.4	19.2	19.7	19.5	18.7
Th/La	0.7	0.8	0.8	0.8	0.8	0.7	0.8	0.7	0.7	0.8
La/Sm	10.1	9.3	9.5	9.6	9.5	9.8	9.6	9.6	9.7	9.8
La/Yb	10.1	10.0	9.6	9.8	10.0	10.4	9.8	10.0	10.1	9.9
U/Th	0.4	0.4	0.3	0.3	0.3	0.3	0.3	0.3	0.3	0.3
Rb/Sr	2.7	3.1	2.4	2.4	2.4	2.2	2.4	2.4	2.3	2.4
Ba/Zr	12.4	19.1	12.2	12.4	12.3	12.0	12.4	12.3	12.1	12.4

* Oxides are renormalised to 100% dry. 1 standard deviation (SD) in brackets

Supplementary Table 5. Representative amphibole analyses

Sample	Christiani CHR 318	Santorini SAN-G	Anafi AN 630	U1589B	U1592B	U1593B	U1598B	U1599A	U1600A
Analyses	7	14	6	23	16	34	21	9	10
SiO ₂	54.64 (0.51)*	55.73 (0.36)	55.35	54.46 (0.43)	54.58 (0.22)	54.68 (0.36)	54.75 (0.27)	54.51 (0.43)	54.92 (0.16)
TiO ₂	0.24 (0.04)	0.19 (0.03)	0.19	0.24 (0.07)	0.20 (0.04)	0.20 (0.04)	0.20 (0.03)	0.21 (0.05)	0.19 (0.03)
Al ₂ O ₃	1.26 (0.14)	1.28 (0.17)	1.21	1.41 (0.34)	1.27 (0.20)	1.28 (0.21)	1.21 (0.13)	1.39 (0.30)	1.17 (0.15)
FeO	16.01 (0.88)	16.17 (0.14)	15.64	16.50 (0.22)	16.45 (0.09)	16.48 (0.19)	16.39 (0.14)	16.37 (0.09)	16.33 (0.11)
MnO	2.25 (0.06)	2.28 (0.05)	2.29	2.31 (0.14)	2.39 (0.04)	2.34 (0.07)	2.35 (0.04)	2.37 (0.05)	2.34 (0.04)
MgO	20.82 (0.35)	20.93 (0.31)	21.11	21.61 (0.34)	22.01 (0.18)	21.80 (0.23)	21.94 (0.18)	21.86 (0.33)	21.89 (0.18)
CaO	1.36 (0.10)	1.41 (0.13)	1.35	1.68 (0.38)	1.31 (0.12)	1.45 (0.24)	1.40 (0.15)	1.45 (0.22)	1.48 (0.11)
Na ₂ O	0.28 (0.04)	0.29 (0.03)	0.28	0.30 (0.07)	0.27 (0.04)	0.27 (0.05)	0.26 (0.03)	0.28 (0.09)	0.25 (0.05)
K ₂ O	0.01 (0.01)	0.00 (0.00)	0.01	0.01 (0.01)	0.01 (0.01)	0.01 (0.01)	0.01 (0.01)	0.01 (0.01)	0.01 (0.01)
Total	96.88	98.27	97.42	98.52	98.47	98.50	98.50	98.44	98.57

Amphibole formulae, recalculated

Christiani	(Na _{0.048} K _{0.002})(Fe _{1.486} Mn _{0.274} Ca _{0.21} Na _{0.03})(Mg _{4.463} Fe ⁱⁱ _{0.439} Al _{0.071})(Si _{7.858} Al _{0.142})O ₂₂ ((OH) ₂)
Santorini	(Na _{0.023})(Fe _{1.456} Mn _{0.273} Ca _{0.214} Na _{0.057})(Mg _{4.417} Fe ⁱⁱ _{0.459} Al _{0.104} Ti _{0.02})(Si _{7.89} Al _{0.11})O ₂₂ ((OH) ₂)
Anafi	(Na _{0.025} K _{0.002})(Fe _{1.465} Mn _{0.277} Ca _{0.206} Na _{0.052})(Mg _{4.486} Fe ⁱⁱ _{0.4} Al _{0.094} Ti _{0.02})(Si _{7.891} Al _{0.109})O ₂₂ ((OH) ₂)
U1589B	(Na _{0.083} Ca _{0.075} K _{0.002})(Fe _{1.541} Mn _{0.278} Ca _{0.181})(Mg _{4.578} Fe ⁱⁱ _{0.42} Ti _{0.001})(Si _{7.739} Al _{0.236} Ti _{0.025})O ₂₂ ((OH) ₂)
U1592B	(Na _{0.027} K _{0.002})(Fe _{1.532} Mn _{0.245} Ca _{0.196} Na _{0.027})(Mg _{4.536} Fe ⁱⁱⁱ _{0.396} Fe ⁱⁱ _{0.068})(Si _{7.582} Fe _{0.227} Al _{0.171} Ti _{0.02})O ₂₂ ((OH) ₂)
U1593B	(Na _{0.037} K _{0.002})(Fe _{1.465} Mn _{0.279} Ca _{0.219} Na _{0.037})(Mg _{4.581} Fe ⁱⁱⁱ _{0.269} Fe ⁱⁱ _{0.15})(Si _{7.707} Al _{0.213} Fe _{0.059} Ti _{0.021})O ₂₂ ((OH) ₂)
U1598B	(Na _{0.036} K _{0.002})(Fe _{1.473} Mn _{0.28} Ca _{0.211} Na _{0.035})(Mg _{4.607} Fe ⁱⁱⁱ _{0.264} Fe ⁱⁱ _{0.128})(Si _{7.713} Al _{0.201} Fe _{0.065} Ti _{0.021})O ₂₂ ((OH) ₂)
U1599A	(Na _{0.038} K _{0.002})(Fe _{1.46} Mn _{0.283} Ca _{0.219} Na _{0.038})(Mg _{4.593} Fe ⁱⁱⁱ _{0.292} Fe ⁱⁱ _{0.114})(Si _{7.683} Al _{0.231} Fe _{0.063} Ti _{0.022})O ₂₂ ((OH) ₂)
U1600A	(Na _{0.034} K _{0.002})(Fe _{1.464} Mn _{0.279} Ca _{0.223} Na _{0.034})(Mg _{4.594} Fe ⁱⁱⁱ _{0.246} Fe ⁱⁱ _{0.16})(Si _{7.732} Al _{0.194} Fe _{0.054} Ti _{0.02})O ₂₂ ((OH) ₂)

* Wt% oxide with 1 standard deviation in brackets

Supplementary Table 6. Representative plagioclase analyses

Sample	Santorini SAN02-25	Anafi ANA18-2	U1589B	U1592B	U1593B	U1598B	U1599A	U1600A
Analyses	13	27	9	11	21	13	22	6
SiO ₂	61.29 (0.39)*	61.43 (0.55)	61.95 (0.61)	61.83 (0.68)	61.49 (0.43)	61.49 (0.36)	61.79 (0.46)	61.66 (0.54)
Al ₂ O ₃	23.71 (0.27)	23.61 (0.38)	24.00 (0.33)	24.13 (0.44)	24.21 (0.17)	24.24 (0.28)	24.10 (0.33)	24.29 (0.27)
CaO	5.52 (0.23)	5.50 (0.39)	5.51 (0.40)	5.67 (0.45)	5.72 (0.17)	5.72 (0.33)	5.57 (0.35)	5.80 (0.27)
FeO	0.19 (0.04)	0.21 (0.03)	0.17 (0.02)	0.17 (0.02)	0.17 (0.01)	0.18 (0.02)	0.16 (0.01)	0.17 (0.01)
Na ₂ O	8.19 (0.15)	8.29 (0.20)	8.17 (0.27)	8.17 (0.23)	7.92 (0.16)	8.08 (0.14)	8.14 (0.17)	7.99 (0.21)
K ₂ O	0.43 (0.03)	0.43 (0.05)	0.44 (0.03)	0.43 (0.03)	0.42 (0.02)	0.42 (0.04)	0.43 (0.04)	0.42 (0.03)
Total	99.33	99.48	100.24	100.40	99.94	100.13	100.19	100.32
An**	26.5	26.2	26.5	27.0	27.9	27.4	26.8	27.9
Ab**	71.1	71.4	71.0	70.5	69.7	70.2	70.8	69.7
Or**	2.5	2.4	2.5	2.4	2.4	2.4	2.5	2.4

* Wt% oxide with 1 standard deviation in brackets

** Percentages of anorthite An (100Ca/[Ca+Na+K]), atomic, albite Ab (100Na/[Ca+Na+K]), and orthoclase Or (100K/[Ca+Na+K]) components.

Supplementary Table 7. Paleobathymetry

Site	Before Archaeos Tuff (m)	After Archaeos Tuff (m)
U1589	200-700	
U1591	200-700	
U1592	500-1000	
U1593	200-700	
U1598	No recovery	200-700
U1599	200-700	
U1600	500-1000	

Supplementary Table 8: Description of the onland facies of the Archaeos Tuff

Christiani	
Outcrop	36°14.74' N / 25°12.53' E. Crops out for 900 m long along the cliffs; maximum 4 m thick
Previous names	Christiani Bims (ref 9) Unterer Bims von Christiani (ref 10), Christiani Ignimbrite (ref 11)
Lithology	Massive to diffusely stratified, poorly sorted lapilli tuff. Nonwelded with the features typical of subaerial ignimbrite. Complex internal stratigraphy with several depositional units. Conspicuous lithic breccia lenses with lithic diameters up to 1 m at the base of the ignimbrite.
Lithics	Perlitic obsidian, basaltic to andesitic lavas, biotite-granites, aplites, greenschists, limestones and marbles
Santorini	
Outcrop	36°22.34' N / 25°25.38' E at the base of the caldera wall near Cape Therma. Two nearby outcrops directly beneath the deposits from the Cape Therma 1 eruption and underlying M1 interplinian deposits
Previous names	Christiani Ignimbrite (ref 11)
Lithology	Massive to diffusely stratified, poorly sorted lapilli tuff. Nonwelded with the features typical of subaerial ignimbrite. Maximum pumice diameters reach 9 cm, with the long axis of the 10 largest pumice clasts ranging from 3.5 to 9.0 cm, and with an average of 5.0 cm. Lithic clasts can be larger than pumices, with the long axis of the 15 largest lithics ranging from 4 to 15 cm, with an average of 8.6 cm.
Lithics	Greenschists, marbles, granitoids, hyaloclastite and variably altered volcanic rocks.
Anafi	
Outcrop	36°21.39' N / 25°48.26'E at 135 m above sea level in the area of Megas Potamos. A single outcrop 10 m long.
Previous names	Christiani Ignimbrite (ref 11)
Lithology	Massive to diffusely stratified, poorly sorted lapilli tuff. Nonwelded with the features typical of subaerial ignimbrite. Lithic clasts are less abundant and on average smaller than in the equivalent deposits on Christiani and Santorini, ranging in size up to only 4 cm (long axis).
Lithics	Lithic clasts are less diverse than on Santorini, with volcanic rocks identified as the principal lithic component.

Supplementary References

- Huijsmans, J.P.P. Calc-alkaline lavas from the volcanic complex of Santorini, Aegean Sea, Greece: a petrological, geochemical and stratigraphic study. *Geologica Ultraiectina* **41**, 316pp (1985).
- Gartzos, E., Dietrich, V.J. & Davis, E. Amphibole-plagioclase fractional crystallisation and magma mixing as major differentiation processes in the Akrotiri Volcanic Complex, Santorini, Greece. *Schweiz. Mineral. Petrogr. Mitt.* **79**, 231-262 (1999).
- Gertisser, R., Preece, K. & Keller, J. The Plinian Lower Pumice 2 eruption, Santorini, Greece: magma evolution and volatile behaviour. *J. Volcanol. Geotherm. Res.* **186**, 387-406 (2009).
- Cantner, K., Carey, S. & Nomikou, P. Integrated volcanologic and petrologic analysis of the 1650 AD eruption of Kolumbo submarine volcano, Greece. *J. Volcanol. Geotherm. Res.* **269**, 28-43 (2014).
- Preine, J., Karstens, J., Hübscher, C., Crutchley, G.J., Druitt, T.H., Schmid, F. & Nomikou, P. The Hidden Giant: How a rift pulse triggered a cascade of sector collapses and voluminous secondary mass-transport events in the early evolution of Santorini. *Basin Res.* **34**, 1465-1485 (2022).
- Fisher, R.V., & Schmincke, H.-U. *Pyroclastic Rocks*. Springer-Verlag, 472pp (1984).
- Jutzeler, M., White, J.D.L., Talling, P.J., McCanta, M., Morgan, S., Le Friant, A. & Ishizuka, O. Coring disturbances in IODP piston cores with implications for offshore record of volcanic events and the Missoula megafloods. *Geochem. Geophys. Geosys.* **15**, 3572-3590 (2014).
- Inman, D.L. Measures for describing the size distribution of sediments. *J. Sediment. Res.* **22**, 125-145 (1952).
- Puchelt, H., Murad, E. & Hubberten, H.W. Geochemical and petrological studies of lavas, pyroclastica and associated xenoliths from the Christiana Islands, Aegean Sea. *Neues Jahrbuch Für Mineralogie-Abhandlungen*, **131**, 140-155 (1977).
- Aarburg, S. & Frechen, M. Die pyroklastischen Abfolgen der Christiana-Inseln (Süd-Ägäis, Griechenland). In Becker-Haumann, R. & Frechen, M. (eds.) *Terrestrische Quartargeologie* 260-276 (1999).
- Keller, J., Dietrich, V., Reusser, E., Gertisser, R. & Aarburg, S. Recognition of a major ignimbrite in the early evolution of the Santorini Group: the Christiani Ignimbrite. *Cities on Volcanoes 6, Tenerife, Spain* pp. 4-5 (Abstract) (2010). <https://www.earth-prints.org/bitstream/2122/6924/1/Cities%20on%20Volcanoes%206%20Abstracts%20Volume.pdf>